Faraday Discussions

Study of electron doping mechanism in single-walled carbon nanotubes using dimethylbenzimidazole

Journal:	*Faraday Discussions*
Manuscript ID	FD-ART-06-2023-000128
Article Type:	Paper
Date Submitted by the Author:	26-Jun-2023
Complete List of Authors:	Tanaka, Naoki; Kyushu University, Applied Chemistry Yamaguchi, Itsuki; Kyushu University Yamaguchi, Ryohei; Kyushu Daigaku Kogakubu Daigakuin Kogakufu, Fujigaya, Tsuyohiko; Kyushu Daigaku Kogakubu Daigakuin Kogakufu,

Study of electron doping mechanism in single-walled carbon nanotubes using dimethylbenzimidazole

N. Tanaka,[a,b] I. Yamaguchi,[a] R. Yamaguchi,[a] and T. Fujigaya*[,a,b,c]

[a] *Department of Applied Chemistry, Graduate School of Engineering, Kyushu University, 744 Motooka, Nishi-ku, Fukuoka 819-0395, Japan*

[b] *International Institute for Carbon Neutral Energy Research (WPI-I²CNER), Kyushu University, 744 Motooka, Nishi-ku, Fukuoka 819-0395, Japan*

[c] *Center for Molecular Systems (CMS), Kyushu University, 744 Motooka, Nishi-ku, Fukuoka 819-0395, Japan*

Keywords: Single-walled carbon nanotube, Electron doping, Reduction, Seebeck coefficient, Proton-coupled electron transfer

Abstract

Single-walled carbon nanotubes (SWCNTs) exhibit p-type properties in air, necessitating electron doping using n-dopants (e.g., reducing agents) for the development of SWCNT-based electronic devices. Dimethylbenzimidazole (DMBI-H) derivatives serve as effective electron dopants not only for SWCNTs but also for various organic semiconducting materials. However, the doping reaction is still a subject of debate. In this study, the electron doping reactions of *ortho*-methoxy-substituted DMBI-H for SWCNTs were analyzed in protic and aprotic solvents in the presence and absence of dioxygen (O_2). The presence of O_2 was found to cause the reduction of O_2 on the SWCNT surface in the protic solvent, resulting in the production of DMBI cations and water through proton-coupled electron transfer (PCET) from the n-doped SWCNT and ethanol. This work elucidates the mechanism behind the air-stability of n-type SWCNTs.

1. Introduction

Single-walled carbon nanotubes (SWCNTs) are attractive materials for various electronics and optoelectronics applications due to their excellent carrier mobility, remarkable thermal conductivity, and broad photoelectron absorption characteristics. To date, numerous applications based on SWCNTs, such as transistors[1-3] and photoelectric conversion,[4, 5] have been developed. Recently, there has been extensive research on the application of SWCNTs for thermoelectric conversion, capitalizing on their significant theoretical Seebeck coefficient and the flexibility of their sheets.[6-8] Carrier doping is performed to control the electronic properties of SWCNTs in these devices. Particularly, since SWCNTs exhibit p-type behavior through hole doping by oxygen and water in the atmosphere, electron doping using electron-donating reagents (n-dopants) has been carried out to prepare n-type SWCNTs. However, it has been pointed out that n-doped SWCNTs are prone to oxidation by dioxygen (O_2) or water (H_2O), leading to poor stability in air atmosphere (less than one month).[9-12] After the discovery of the first stable n-type SWCNT doped with the crown ether/NaOH system in 2016, [13] several n-dopants such as polyethyleneimine (PEI)[14-16] and guanidinium salts[17] were reported, offering stable n-doped SWCNTs that exhibited air stability for more than one month. It was suggested that the key requirement for stability is the formation of stable cations upon doping, which interact with the negatively-charged SWCNTs. However, the mechanism of this stability has not been extensively studied.

In 2017, we discovered that dimethylbenzimidazole (DMBI-H) derivatives (**Fig. 1a**), which are conventionally used as n-dopants for organic semiconductors,[18-22] also provided n-type SWCNTs with excellent stability in the air atmosphere.[23] We revealed the importance of multilayer coverage by dopant cations to achieve stability.[20] Interestingly, we observed that DMBI-H in the solution was quantitatively converted to DMBI cations after 24 hours, while no such reaction was observed in the absence of SWCNTs.[20] Considering that DMBI cations strongly interact with negatively-charged SWCNTs via Coulombic interaction, the detection of

DMBI cation in the bulk solution suggested the occurrence of unknown reactions. Elucidating these reactions may help understand the mechanism of multilayer adsorption that leads to excellent stability.

Herein, we investigated the formation mechanism of DMBI cations in the bulk solution after doping SWCNTs and examined the relationship between the stability of n-doped SWCNTs and the reactions of DMBI-H. Recently, Wang et al. reported that the proton-coupled electron transfer (PCET) of DMBI-H activates O_2 in the presence of a protic acid, resulting in the production of hydrogen peroxide (H_2O_2) and water (H_2O) without the formation of a high-energy superoxide radical anion (O_2^-).[24] Based on this finding, we speculated that PCET occurs during the doping process, catalyzed by the n-doped SWCNTs as an electron source and ethanol as a proton source, leading to O_2 activation. Therefore, the redox reaction of DMBI in protic and aprotic solvents was studied in the absence and presence of O_2. As a result, we found that the O_2 reduction reaction effectively proceeds in ethanol, producing H_2O and DMBI cations (**Fig. 1b**). Conversely, these reactions did not occur in toluene, and the resulting n-type SWCNT sheets exhibited poor air stability. Based on these results, we discussed the SWCNT doping mechanism of DMBI-H.

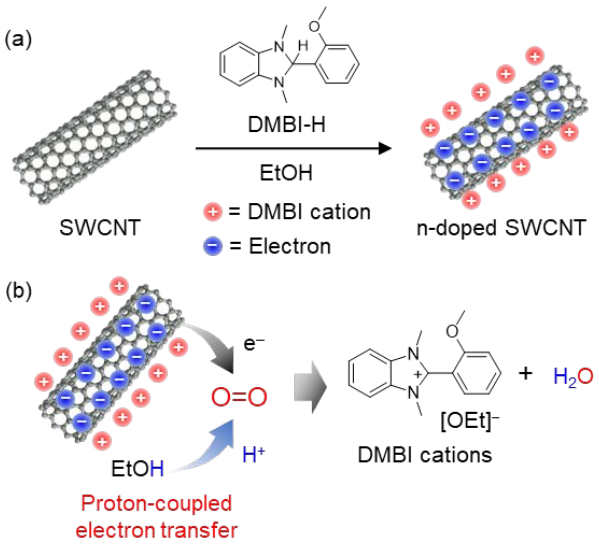

Fig. 1 (a) Electron doping of SWCNT by DMBI-H in ethanol. (b) O_2 activation by proton-coupled electron transfer using n-doped SWCNT and ethanol.

2. Result and Discussion

Single-walled carbon nanotube (SWCNT; average diameter of 1.5 nm) sheets were prepared by filtering a SWCNT dispersion in *N*-methylpyrrolidone (NMP). The resulting sheets, with a thickness of approximately 10 μm, were utilized for the doping experiments. The obtained SWCNT sheets (4 mm × 15 mm) were immersed in deuterated ethanol (ethanol-d_5) solutions of DMBI-H (30 mM) for 24 hours, and the solutions were collected for ^{1}H NMR measurements. Blank experiments were also conducted without using SWCNT sheets. Fig. 2a shows a comparison of the ^{1}H NMR spectra in ethanol-d_5. In the presence of SWCNT sheets, new peaks at 7.47, 7.86, and 8.05 ppm in the aromatic region, attributable to the DMBI cation, were observed (Fig. 2b, red line), whereas these peaks were very weak in the absence of SWCNT sheets (Fig. 2b, blue line). Based on the integral ratio of the peak at 8.05 ppm (DMBI cation) to that at 6.60 ppm (DMBI-H), the amount of DMBI cations was estimated to be 34% in the presence of SWCNTs, which is significantly higher than that in the solution without SWCNT sheets (8%). This indicates the involvement of SWCNTs in the formation reaction of DMBI cations. On the other hand, control experiments using ethanol-d_5 degassed with N_2 only showed a DMBI cation content as low as ~3%, even in the presence of SWCNT sheets, suggesting that O_2 is also essential for the formation of DMBI cations in the bulk solution (Fig. S1). To compare the reactions in an aprotic solvent, the same doping experiments were also performed in toluene-d_3. Interestingly, as observed in the ^{1}H NMR spectra, the peaks of the DMBI cation were not detected both with (Fig. 2b, red line) and without (Fig. 2b, blue line) SWCNT sheets, even in the presence of O_2. It should be noted that new peaks derived from the DMBI oxidant (DMBI-Ox)[25, 26] appeared when the toluene solutions of DMBI were left for another 2 weeks (Fig. S2).

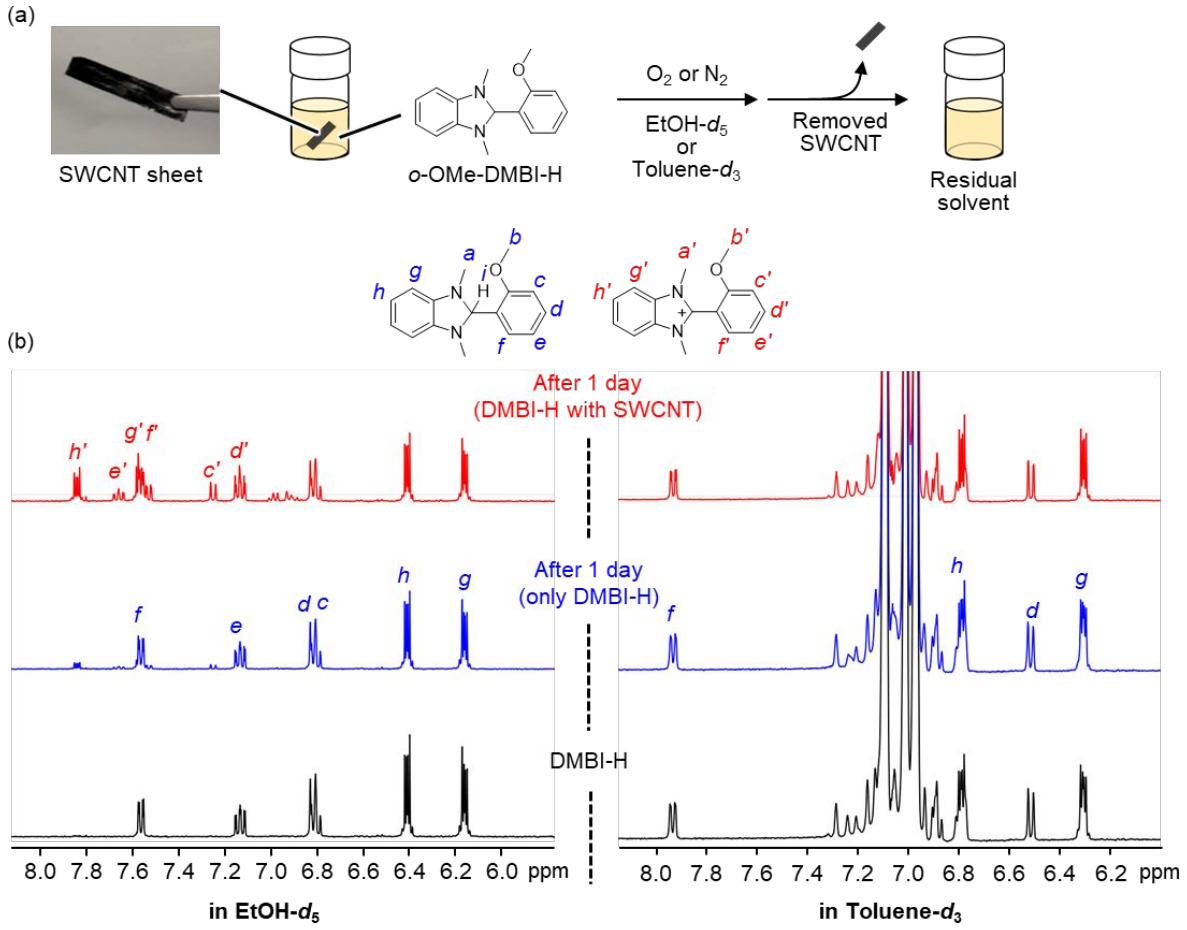

Fig. 2 (a) Experimental procedure for evaluation of DMBI cation content by ^{1}H NMR measurement. (b) ^{1}H NMR spectra in EtOH-d_5 and toluene-d_3 of residual solvent after SWCNT doping with DMBI-H for 24 hours (red line), a solution of DMBI-H after 24 hours (blue line), and a solution of DMBI-H (black line).

The SWCNT sheets obtained from the doping process were subjected to Seebeck coefficient and electrical conductivity measurements. Figure 3a illustrates the change in Seebeck coefficient of SWCNT sheets doped in ethanol (30 mM) and toluene (30 mM) at 30 °C in the presence of O_2. Immediately after doping, the SWCNT sheet doped in ethanol exhibited a negative Seebeck value of -31.7 μV K^{-1}, while the one doped in toluene showed -44.4 μV K^{-1}, indicating their n-type nature. Although no DMBI cations were detected in the bulk toluene-d_3 solution, as shown in Fig. 2b, the negative Seebeck value clearly indicated the doping reaction

still occurred. We speculate that DMBI-H transferred electrons to SWCNT in toluene, forming DMBI cations, but these cations remained strongly bound to the surface due to Coulombic interaction. Interestingly, we found that the SWCNT sheets doped in ethanol remained n-type for more than 50 days, as previously reported,[20] while the ones doped in toluene reverted to p-type after 20 days. In our previous study, we established through adsorption isotherm measurements that the multilayer adsorption of DMBI cations is crucial for achieving long-term stability in the air atmosphere. Therefore, the poor stability observed in the SWCNT sheets doped in toluene suggests that the SWCNTs were not sufficiently coated by DMBI cations in toluene.

Regarding electrical conductivity, the SWCNT sheets doped in ethanol exhibited a value of 1×10^5 S m^{-1}, whereas the sheets doped in toluene showed 4×10^4 S m^{-1} (Fig. 3b). These results indicate that a larger number of electrons were injected when ethanol was used as the solvent. We observed a drop in electrical conductivity for the sheet doped in ethanol, while only a slight drop was observed for the sheet doped in toluene. Large drops at the beginning of the monitoring were often observed,[23] although the detailed mechanism behind this phenomenon has not been clarified yet.

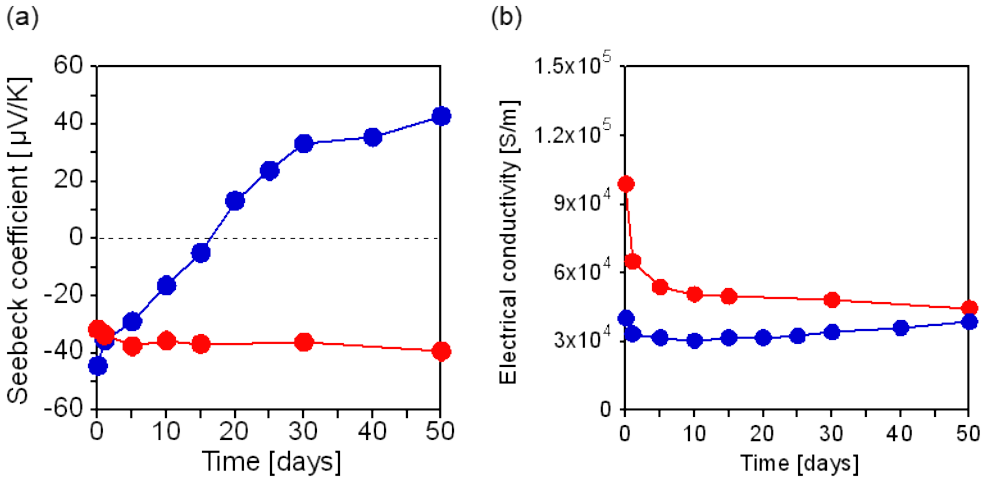

Fig. 3 (a) Seebeck coefficient and (b) electrical conductivity of the SWCNT sheets dipped in the 30-mM DMBI-H solutions in ethanol (red line) and in toluene (blue line).

The water content in dehydrated ethanol was evaluated using Karl Fischer measurements two weeks after the doping process (Table 1). In the absence of O_2, the increase in H_2O content in the DMBI-H solution, with and without SWCNT sheets, was only 8% and 14%, respectively. However, in the presence of O_2, the water content increased by 170% when SWCNT sheets were doped, clearly indicating the utilization of O_2 for H_2O production. It is worth noting that in the absence of SWCNT sheets, H_2O increased by 114%. Recently, Wang et al. reported the proton-coupled electron transfer (PCET) of DMBI-H activated O_2 and generated H_2O_2 and H_2O using a protic acid.[24] Therefore, we considered that ethanol acted as a proton source and a similar PCET of DMBI-H took place in our system.

Fig. 4 illustrates the absorption spectra of ethanol after two weeks of doping. In the presence of O_2 (red lines in Fig. 4), an absorption peak at 280 nm, characteristic of the spectra of DMBI cations, was observed.[20] Particularly, a higher intensity at 280 nm was observed when the SWCNT sheets were doped, suggesting that SWCNTs accelerate the formation of DMBI cations. On the other hand, in the absence of O_2, the spectra were almost similar to that of pure DMBI-H, both with and without SWCNT sheets, indicating that O_2 is necessary for the generation of DMBI cations in the bulk solution.

Table 1. Change of the water content of ethanol solvent after doping of SWCNT with DMBI-H for 2 weeks.

Condition		0 day	14 days
Under N_2	SWCNT/DMBI	593 ppm	643 ppm
	DMBI only	585 ppm	670 ppm
Under O_2	SWCNT/DMBI	550 ppm	1485 ppm
	DMBI only	552 ppm	1184 ppm
Under N_2	EtOH solvent	13.3 ppm	95.5 ppm

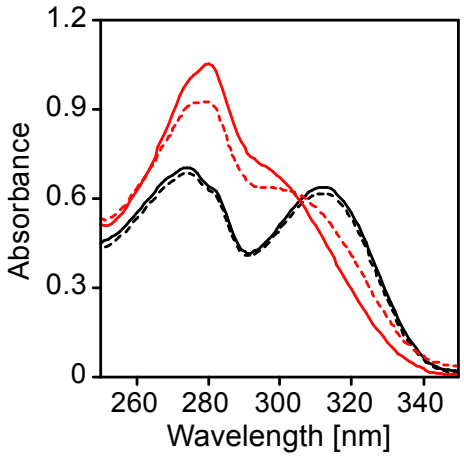

Fig. 4 Absorption spectra of ethanol solutions after two weeks of SWCNT doping (red line) and DMBI only (dashed red line) in the presence of O_2. Absorption spectra of ethanol solutions after two weeks of SWCNT doping (black line) and DMBI only (dashed black line) in the absence of O_2.

It has been widely accepted that electron transfer occurs from the highest occupied molecular orbital (HOMO) of DMBI-H to the conduction band of the semiconductors,[27, 28] followed by C-H bond cleavage of the imidazole backbone.[28-32] Based on the above experimental results together with the reported mechanisms, we have summarized the mechanism of electron doping of SWCNTs by DMBI-H in Fig. 5.

Step 1: Electron transfer from DMBI-H to SWCNT (Fig. 5a (1)): Although the calculated HOMO energy of DMBI-H is –4.46 eV, which is lower than the conduction band of SWCNTs (–4.2 eV) under vacuum conditions,[20] p-type SWCNT doped by adsorbed O_2 decreases the energy level of the conduction band. Thus, electron transfer from DMBI-H to SWCNT readily occurs, forming a DMBI cation/SWCNT complex by generating OOH radicals (Fig. 5b).

Step 2: Generation of DMBI radical (Fig. 5a (2)): The produced OOH radicals are immediately converted to H_2O_2 by abstracting hydrogen atoms from DMBI-H, resulting in DMBI radicals that have high singly occupied molecular orbital (SOMO) levels (–2.53 eV).

Step 3: Electron transfer from DMBI radical to SWCNTs (Fig. 5a (3)): Electron transfer from DMBI radical to SWCNT occurs until the SOMO level, resulting in the conversion of SWCNT into n-type (Fig. 5b).[20]

Step 4: PCET reaction with O_2 and ethanol (Fig. 5 (4)): When the solvent is ethanol, O_2 activation by PCET proceeds with ethanol as a proton source and n-doped SWCNTs as an electron source, providing OOH radicals. As the electrons are used for PCET, counter cations (e.g., DMBI cation) adsorbed on the SWCNT surface dissolve into the bulk solution. The generated OOH radicals react with DMBI-H to form H_2O_2, and DMBI radical can further be used for doping of SWCNTs (Fig. 5 (2)). In this step, the concentration of DMBI cation in the bulk solution increases, and some of them adsorb onto the SWCNT surface to form multilayer adsorption. Such excess adsorption of DMBI cation contributes to the barrier for oxidation. This step does not take place in the toluene solution due to the lack of acidic protons, but the generation of DMBI-Ox takes place instead as reported.[29]

Step 5: PCET reaction with H_2O_2 and ethanol (Fig. 5 (5)): With an increased concentration of H_2O_2, the PCET reaction produces water (Fig. 5b). Since the PCET reaction occurs through DMBI-H,[24] direct H_2O production is possible, but the PCET through SWCNT occurs faster, probably due to the effective adsorption of O_2 onto SWCNTs. Therefore, n-doped SWCNT sheets can act as catalysts for the oxygen reduction reaction.

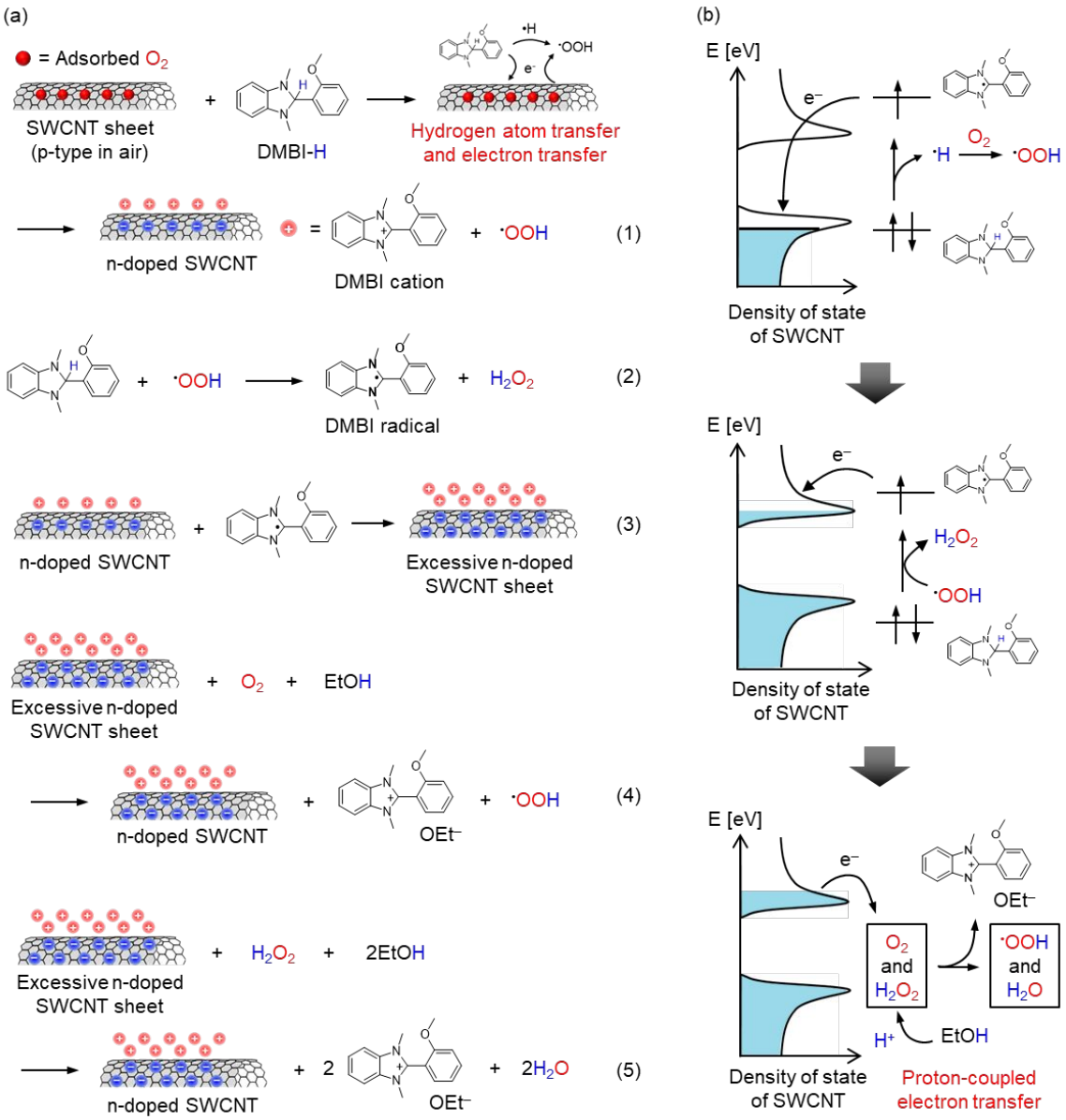

Fig. 5 (a) Proposed mechanism and (b) change of electric state of SWCNT for electron doping of SWCNT by DMBI-H in ethanol.

3. Conclusion

In this study, we explored the doping mechanism of SWCNTs using DMBI-H by comparing the monitoring of DMBI cations in the bulk solution and the amount of H_2O produced after doping under various reaction conditions. Doping with ethanol under an oxygen atmosphere significantly increased the amount of DMBI cations and water compared to the blank experiments without SWCNT sheets. On the other hand, when toluene was used as the solvent,

although n-doping of the SWCNT sheet occurred, DMBI cation was not detected in the bulk solution, and the sheets were less stable in air, indicating that the amount of DMBI cations covering the SWCNT surface was less than that of the doped sheets in ethanol. Based on these results, we concluded that the doping of SWCNTs with DMBI-H in ethanol is expected to proceed through PCET-based reduction of O_2, with n-type SWCNTs serving as the electron source and ethanol as the proton source, converting all DMBI-H into DMBI cations. This study significantly contribute to the mechanism study of air-stable n-type SWCNT as well as reaction mechanism of organic dopants.

4. Experimental Section

Materials: SWCNTs (Meijo-eDIPS) with a diameter of 1.5 ± 0.5 nm were purchased from Meijo Nano Carbon. *N*-methylpyrrolidone (NMP), methanol, ethanol-d_5, toluene-d_8 were purchased from FUJIFILM Wako Pure Chemicals Corp (Tokyo, Japan).

Characterization: ^{1}H NMR spectra were recorded using a JEOL JNM-ECZ400 (400 MHz). UV-vis absorption measurements were performed using a V-670 spectrophotometer (JASCO, Tokyo Japan). The in-plane electrical conductivity and in-plane Seebeck coefficient were measured using a ZEM-3 measurement system (ADVANCE RIKO, Yokohama Japan) under the atmosphere from 30 °C. Water contents in the ethanol solution were measured by Karl Fischer titration (Kyoto, Electronics, Japan).

Fabrication of SWCNT sheets: SWCNTs (5.0 mg) were dispersed in NMP (40 mL) using a bath-type sonicator (Branson 5010) for 1 hour. The dispersion through a Pasteur pipette cotton plug to remove agglomerated SWCNTs. SWCNT sheets were obtained by filtering the dispersion through a polytetrafluoroethylene membrane (diameter: 90 mm, pore size: 0.2 μm). SWCNT sheets were washed by dipping them in methanol to remove residual NMP, followed by vacuum-drying at 80 °C for 8 hours. The thickness of the films was around 10±5 μm.

Acknowledgements

This work was supported by Data Creation and Utilization-Type Material Research and Development Project (Grant Number JPMXP1122714694) of the MEXT, and Advanced Research Infrastructure for Materials and Nanotechnology in Japan (ARIM) of the MEXT (Grant Number JPMXP1222KU1007). T. F. thanks Core Research for Evolutional Science and Technology (CREST) (No. JPMJCR19Q5) from the Japan Science and Technology Agency (JST). N. T. thanks to ACT-X (No. JPMJAX21KB) from JST.

References

1. A. D. Franklin and Z. Chen, *Nat Nanotechnol*, 2010, **5**, 858-862.
2. B. N. Khare, P. Wilhite, R. C. Quinn, B. Chen, R. H. Schingler, B. Tran, H. Imanaka, C. R. So, C. W. Bauschlicher, Jr. and M. Meyyappan, *J. Phys. Chem. B*, 2004, **108**, 8166-8172.
3. B. Akdim, X. Duan, D. A. Shiffler and R. Pachter, *Materials Research Society Symposium Proceedings*, 2003, **800**, 339-347.
4. Z. Yang, L. Li, Y. Luo, R. He, L. Qiu, H. Lin and H. Peng, *J. Mater. Chem. A*, 2013, **1**, 954-958.
5. Y. Luo, X. Li, J. Zhang, C. Liao and X. Li, *J. Nanomater.*, 2014, **2014**, 1-13.
6. J. L. Blackburn, A. J. Ferguson, C. Cho and J. C. Grunlan, *Adv Mater*, 2018, **30**.
7. B. Kumanek, G. Stando, P. Stando, K. Matuszek, K. Z. Milowska, M. Krzywiecki, M. Gryglas-Borysiewicz, Z. Ogorzalek, M. C. Payne, D. MacFarlane and D. Janas, *Sci. Rep.*, 2021, **11**, 8649.
8. C. Meng, C. Liu and S. Fan, *Adv Mater*, 2010, **22**, 535-539.
9. K. S. Mistry, B. A. Larsen, J. D. Bergeson, T. M. Barnes, G. Teeter, C. Engtrakul and J. L. Blackburn, *ACS Nano*, 2011, **5**, 3714-3723.
10. J. B. Bult, R. Crisp, C. L. Perkins and J. L. Blackburn, *ACS Nano*, 2013, **7**, 7251-7261.
11. P. G. Collins, K. Bradley, M. Ishigami and A. Zettl, *Science*, 2000, **287**, 1801-1804.
12. C. Yu, A. Murali, K. Choi and Y. Ryu, *Energy Environ. Sci*, 2012, **5**, 9481-9486.
13. Y. Nonoguchi, M. Nakano, T. Murayama, H. Hagino, S. Hama, K. Miyazaki, R. Matsubara, M. Nakamura and T. Kawai, *Adv. Funct. Mater.*, 2016, **26**, 3021-3028.
14. M. Rdest and D. Janas, *Materials (Basel)*, 2020, **14**.
15. Y. Ni, H. Hu, B. Malarkey Erik, B. Zhao, V. Montana, C. Haddon Robert and V. Parpura, *J. Nanosci. Nanotechnol.*, 2005, **5**, 1707-1712.
16. C. Yu, A. Murali, K. Choi and Y. Ryu, *Energy & Environmental Science*, 2012, **5**.
17. S. Horike, Q. Wei, K. Akaike, K. Kirihara, M. Mukaida, Y. Koshiba and K. Ishida, *Nat Commun*, 2022, **13**, 3517.
18. Q. Hu, Z. Lu, Y. Wang, J. Wang, H. Wang, Z. Wu, G. Lu, H.-L. Zhang and C. Yu, *J. Mater. Chem. A*, 2020, **8**, 13095-13105.
19. R. Yamaguchi, T. Ishii, M. Matsumoto, A. Borah, N. Tanaka, K. Oda, M. Tomita, T. Watanabe and T. Fujigaya, *J. Mater. Chem. A*, 2021, **9**, 12188-12195.

20. Y. Nakashima, R. Yamaguchi, F. Toshimitsu, M. Matsumoto, A. Borah, A. Staykov, M. S. Islam, S. Hayami and T. Fujigaya, *ACS Appl. Nano Mater.*, 2019, **2**, 4703-4710.
21. Y. Nakashima, N. Nakashima and T. Fujigaya, *Synthetic Metals*, 2017, **225**, 76-80.
22. H. Wang, P. Wei, Y. Li, J. Han, H. R. Lee, B. D. Naab, N. Liu, C. Wang, E. Adijanto, B. C. Tee, S. Morishita, Q. Li, Y. Gao, Y. Cui and Z. Bao, *Proc. Natl. Acad. Sci. U. S. A.*, 2014, **111**, 4776-4781.
23. Y. Nakashima, N. Nakashima and T. Fujigaya, *Synth. Met.*, 2017, **225**, 76-80.
24. Y. F. Wang and M. T. Zhang, *J. Am. Chem. Soc.*, 2022, **144**, 12459-12468.
25. N. Tanaka, T. Ishii, I. Yamaguchi, A. Hamasuna and T. Fujigaya, *J. Mater. Chem. A*, 2023, **11**, 6909-6917.
26. S. Zhang, B. D. Naab, E. V. Jucov, S. Parkin, E. G. Evans, G. L. Millhauser, T. V. Timofeeva, C. Risko, J. L. Bredas, Z. Bao, S. Barlow and S. R. Marder, *Chemistry (Easton)*, 2015, **21**, 10878-10885.
27. Y. Lu, Z. D. Yu, R. Z. Zhang, Z. F. Yao, H. Y. You, L. Jiang, H. I. Un, B. W. Dong, M. Xiong, J. Y. Wang and J. Pei, *Angew. Chem. Int. Ed. Engl.*, 2019, **58**, 11390-11394.
28. D. Huang, H. Yao, Y. Cui, Y. Zou, F. Zhang, C. Wang, H. Shen, W. Jin, J. Zhu, Y. Diao, W. Xu, C. A. Di and D. Zhu, *J. Am. Chem. Soc.*, 2017, **139**, 13013-13023.
29. O. Bardagot, C. Aumaître, A. Monmagnon, J. Pécaut, P.-A. Bayle and R. Demadrille, *Appl. Phys. Lett.*, 2021, **118**.
30. Y. Zeng, W. Zheng, Y. Guo, G. Han and Y. Yi, *J. Mater. Chem. A*, 2020, **8**, 8323-8328.
31. S. Riera-Galindo, A. Orbelli Biroli, A. Forni, Y. Puttisong, F. Tessore, M. Pizzotti, E. Pavlopoulou, E. Solano, S. Wang, G. Wang, T. P. Ruoko, W. M. Chen, M. Kemerink, M. Berggren, G. di Carlo and S. Fabiano, *ACS Appl Mater Interfaces*, 2019, **11**, 37981-37990.
32. B. D. Naab, S. Guo, S. Olthof, E. G. Evans, P. Wei, G. L. Millhauser, A. Kahn, S. Barlow, S. R. Marder and Z. Bao, *J. Am. Chem. Soc.*, 2013, **135**, 15018-15025.